Journal of Rock Mechanics and Geotechnical Engineering 11 (2019) 824–836

Contents lists available at ScienceDirect

Journal of Rock Mechanics and Geotechnical Engineering

journal homepage: www.rockgeotech.org

Full Length Article

Monotonic, cyclic and post-cyclic performances of single-helix anchor in residual soil of sandstone

José Antonio Schiavon [a,b,*], Cristina de Hollanda Cavalcanti Tsuha [b], Luc Thorel [c]

[a] Department of Geotechnical Engineering, Aeronautics Institute of Technology, São José dos Campos, Brazil
[b] Department of Geotechnical Engineering, University of São Paulo, São Carlos, Brazil
[c] IFSTTAR, GERS Department, Geomaterials & Models in Geotechnics Laboratory, Bouguenais, France

ARTICLE INFO

Article history:
Received 20 August 2018
Received in revised form
21 November 2018
Accepted 24 December 2018
Available online 30 March 2019

Keywords:
Helical anchors
Tropical residual soil
Cyclic loading
Field load tests

ABSTRACT

Helical anchors are commonly used in Brazil for guyed transmission towers subjected to static and cyclic wind loads. In most cases, these anchors are installed in tropical residual soil, a micro-structured material in which the shear strength is provided by soil bonding. During installation of a helical anchor, as the helical plate moves downward into the ground, the soil penetrated is sheared and displaced. Consequently, in this type of soil, anchor installation affects the soil shear strength significantly associated with a bonded structure. However, the cyclic responses of helical anchors in this type of structured soils are rarely reported. To address this problem, tests were conducted in a Brazilian residual soil to investigate the monotonic, cyclic and post-cyclic performances of single-helix anchors. Field tests used two instrumented single-helix anchors installed in this typical residual soil of sandstone, which is frequently observed in large areas in the southern Brazil. The testing results indicate that the disturbance caused by the anchor installation affected the monotonic uplift performance markedly. The results of cyclic loading tests also show no significant degradation of helix bearing resistance and reduced displacement accumulation with increasing load cycles. This is perhaps due to the soil improvement caused by previous loading, which then increases the stiffness response of the anchor.

1. Introduction

In Brazil, one of the main challenges is the electricity transmission demand. The Brazilian National Interconnected System (SIN) for generation and transmission of electricity includes approximately 129,000 km of transmission lines crossing various sites of different geotechnical conditions. In this context, the use of helical anchors to support guyed transmission towers has increased markedly in recent years, although a significant number of towers have been installed in areas of tropical residual soils.

In most countries across the world, residual soils occur generally in tropical regions, where heavy rainfall and warm temperatures are favourable to chemical weathering, which results in deep residual soil profiles (Townsend, 1985). Mineralogical content and structure are the two major properties that can lead to distinctive characteristics of residual soils (Wesley, 2009). The term 'structure' refers to as the inter-particle bonding and cementation of residual soil in undisturbed condition. Causes of inter-particle bonding include relics of parent rock, recrystallization of minerals during weathering, and precipitation of salts from pore water (Mitchell and Sitar, 1982). Inter-particle bonding provides a component of strength and stiffness that are eliminated or destroyed by remoulding the soil in its undisturbed condition. Therefore, the changes in the structure of residual soils caused by anchor installation may play an important role in the uplift responses of helical anchors.

Kulhawy (1985) stated that significant disturbance does occur within the cylindrical zone penetrated by the helical anchor during installation. Soil structure alterations caused by installation of helical anchors in different soils have been extensively discussed (e.g. Nagata and Hirata, 2005; Wang et al., 2010; Tsuha et al., 2012; Weech and Howie, 2012; George and Clemence, 2013; Bagheri and El Naggar, 2015; Lutenegger and Tsuha, 2015; Pérez et al., 2018). The effect of helical anchors on the uplift capacity of highly porous structured residual soil (of diabase rock) was investigated experimentally in Tsuha et al. (2016). Their results demonstrated

* Corresponding author. Fax: +55 12 39476801.
E-mail address: schiavon@ita.br (J.A. Schiavon).

Peer review under responsibility of Institute of Rock and Soil Mechanics, Chinese Academy of Sciences.

https://doi.org/10.1016/j.jrmge.2018.12.012

that the installation of single- and multi-helix helical anchors caused significant breakdown of natural soil bonding and consequently reduced uplift capacity was noticed. To the authors' knowledge, this is one of few studies that have examined the static performances of helical anchors in a tropical residual soil. Unfortunately, no studies on the cyclic and post-cyclic responses of helical anchors in tropical residual soils have been published in the time of writing, although application of helical anchors in Brazil is mainly used as foundation reinforcement of guyed transmission towers, for which the cyclic wind load is the major design load. For this, the current investigation studied the cyclic and post-cyclic performances of single-helix anchors in a tropical residual soil of sandstone, through conducting a series of monotonic and cyclic field load tests, in order to provide useful information on the design of anchors for guyed towers in residual soils.

1.1. Past studies on the cyclic performances of helical anchors

The loading and unloading cycles experienced by helical anchors during their service life in guyed towers can modify the soil characteristics around the anchor, mainly in the zone of disturbed soil above the helix. Consequently, the helical anchor performance may change with wind loading cycles.

Cerato and Victor (2009) conducted full-scale cyclic tests on helical anchors, and observed that triple-helix anchors exhibited low displacement accumulation under cyclic loading carried out after the seating load. The triple-helix anchors were installed with the top helix at depths of 16.5D and 18D (D is the helix diameter) in a layer of silty clay with sand, subjected to cyclic loading with a maximum cyclic load (Q_{max}) up to 50% of the predicted uplift capacity (Q_T). On the other hand, the double-helix anchor installed in a sand layer with the top helix at depth of 13.8D showed continuous displacement accumulation for at least 1×10^6 load cycles varying from $0.11Q_T$ to $0.22Q_T$ (cycles with frequency of 3 Hz for 100 h). Buhler and Cerato (2010) noticed that the cyclic load amplitude ($Q_{max} - Q_{min}$) has a greater influence rather than Q_{max} on the helical anchor response at loads significantly less (~50%) than the predicted Q_T.

Newgard et al. (2015) observed significant displacement accumulation followed by complete anchor pullout, during cyclic model tests on shallow single-helix anchors in sand. In their tests, the helical anchor models were subjected to a very low minimum cyclic load (Q_{min}) and large cyclic load amplitude of up to $0.6Q_T$. The shallow helix embedment depth (between 3D and 5.6D) and low Q_{min} may have contributed to the flow of sand toward the void created beneath the helical plate due to the increasing cyclic upward movement, which led to decrease in horizontal stress around the helix and degradation of the helix uplift resistance. In contrast, Schiavon et al. (2017) observed decrease (but not cease) in the rate of displacement accumulation and no sudden pullout for a number of tensile load cycles carried out on helical anchor models in sand at 7.4D of helix depth (H), in a centrifuge test. While Newgard et al. (2015) tested the anchor models between 1155 and 9506 load cycles, respectively, for 3D and 5.6D helix depths, with cyclic load amplitude of ~$0.58Q_T$, Schiavon et al. (2017) carried out cyclic tests with 300, 1000 and 2000 load cycles for cyclic load amplitudes of $0.68Q_T$, $0.58Q_T$ and $0.4Q_T$, respectively. Although fewer cycles have been conducted in Schiavon et al. (2017), displacement accumulation regime and cyclic pullout seem to be significantly influenced by helix depth (H), cyclic load amplitude and minimum cyclic load (Q_{min}).

Fahmy and El Naggar (2016) investigated the cyclic response of anchors previously subjected to both monotonic and cyclic loads. In full-scale tests on single-helix anchors with tapered shaft in sand with silt, a detrimental effect was observed on anchor cyclic performance due to the prior monotonic uplift loading. Larger cyclic displacement was the result of decrease in the confining pressure acting on the shaft and the likely gap opening and soil cave-in below the helical plate (Fahmy and El Naggar, 2016). In addition, Fahmy and El Naggar (2016) observed significant accumulated displacement for the helical anchor re-tested at greater cyclic loading amplitude.

Costa (2017) conducted five series of tests on two triple-helix anchors installed in sand with the bottom helix at depths of 7.1D and 7.9D, respectively, in Northeast Brazil, each test series having 50 cycles with different cyclic load amplitudes. Greater displacement accumulation was observed approximately in the first 10 cycles of all series, due to the disturbed condition of the soil above the helical plates (installation effect). The first load 10 cycles changed the soil density, and thus increased soil stiffness. For the cyclic test with $Q_{max} = 0.77Q_T$, the rate of displacement accumulation showed an increasing trend with cycles, having a notably large displacement accumulation for the last cycles and a clear trend upon anchor pullout.

Schiavon et al. (2018) evaluated the influence of two cyclic loading series with different cyclic load amplitudes via centrifuge tests. The helical anchor model subjected to a sequence of low–high cyclic load amplitude exhibited nearly 40% greater accumulated displacement than that under the high–low cyclic load amplitude. According to Cerato and Victor (2009), a cyclic preloading programme for anchor should be implemented in order to properly seat the anchors and ensure the desired lifetime performance.

1.2. Past studies on the post-cyclic performances of helical anchors

Trofimenkov and Mariupolskii (1965) observed that the influence of one-way cyclic loading on helical anchors depends on the soil properties. For anchors in medium-hard clays, the post-cyclic capacity was about 70%–80% of the values obtained in pre-cyclic tests. In contrast, the post-cyclic capacity of helical anchors in saturated sand was approximately 60%–70% of the pre-cyclic ultimate capacity.

From reduced tests on 1g-scale models in clay, Narasimha Rao and Prasad (1991) observed that cyclic loading with Q_{max} up to $0.3Q_T - 0.4Q_T$ caused mainly elastic displacements, and no apparent reduction was observed with respect to the uplift capacity with Q_{max} values up to $0.55Q_T$. For greater Q_{max} ($=0.7Q_T$–$0.8Q_T$), a decrease in the uplift capacity of approximately 8%–34% was observed. In addition, Narasimha Rao and Prasad (1991) suggested that the cyclic behaviour of deep anchors seems to be better than that of shallow anchors.

According to the past researches on plate anchor models under cyclic loading, Clemence and Smithling (1984) reported that helical anchor models in sand experienced degradation of anchor capacity with increasing cycle number. Although stress cell measurements showed increase in horizontal stress during installation, the anchor movement during cyclic loading caused relaxation of horizontal stresses, which explains the degradation of uplift capacity.

The post-cyclic monotonic loading results presented by Newgard et al. (2015) also showed degradation of ultimate capacity of shallow helical anchor models in sand. For cyclic tests with cyclic load amplitude ($Q_{max} - Q_{min}$) of approximately $0.21Q_T$ and $0.52Q_T$, the reduction in the post-cyclic monotonic capacity was 12% and 26%, respectively.

On the other hand, Cerato and Victor (2009) proposed that cyclic loading at relatively high cyclic load/static uplift capacity ratios (from 0.25 to 0.4) may increase considerably the helical anchor uplift capacities. Centrifuge tests conducted by Schiavon et al. (2017) showed no degradation of post-cyclic monotonic capacity

for helical anchor models in sand subjected previously to cyclic load amplitude between $0.4Q_T$ and $0.68Q_T$. On the contrary, the anchor model subjected to greater cyclic load amplitude ($0.68Q_T$) previously showed a post-cyclic capacity of 5% greater than the pre-cyclic monotonic value. After five series of cyclic tests with 50 load cycles, in which the helical anchor was subjected to Q_{max} up to $0.51Q_T$, Costa (2017) observed greater monotonic capacity and significantly stiffer response. For an upward displacement equivalent to 10% of the mean helix diameter, the post-cyclic uplift capacity was 7%–40% greater than that of the helical piles tested only monotonically. Schiavon et al. (2018) observed that the most significant degradation of post-cyclic capacity occurred for helical anchors that exhibited stable cyclic response in cyclic load test (accumulated displacements $< 0.1D$ after 1000 cycles). Therefore, they suggested that the design of helical anchors subjected to cyclic loading should take into account both the displacement accumulation regime and the post-cyclic capacity degradation.

2. Testing programme

Two single-helix anchors were installed and subjected to a set of full-scale load tests at the Experimental Foundations Site of the São Carlos School of Engineering, University of São Paulo, Brazil. The anchors had the shaft instrumented with strain gauges just above the helix in order to separate the helix bearing and shaft resistance.

During the lifetime of a guyed transmission tower, the maximum wind load is less frequently observed (few or sparse occurrence). In addition, in periods between two events of the maximum load, cyclic loading of lower amplitude normally occurs. Therefore, to simulate a scenario in which the helical anchor is subjected to single ultimate load cycles combined with a series of intermediate low-amplitude load cycles, the single-helix anchor termed as 1CHA was subjected to a set of monotonic (ultimate load cycle) and cyclic uplift tests (Fig. 1). On the other hand, the anchor termed as 1MHA was submitted solely to monotonic load tests (series of ultimate load tests). The aim of these tests was to distinguish the influence of a prior ultimate load cycle and of a prior cyclic loading with different amplitudes on the post-cyclic uplift capacity of the anchor.

2.1. Testing site

The testing site is located at São Carlos City, the central region of the state of São Paulo, Southeast Brazil (Fig. 2). São Carlos City lies on the Upper Jurassic–Lower Cretaceous sandstones and Cretaceous migmatites, approximately 230 km far from São Paulo City (the largest city in Brazil). Above these rocks, Mesozoic sandstones and conglomerates and Cenozoic sediments cover the whole region.

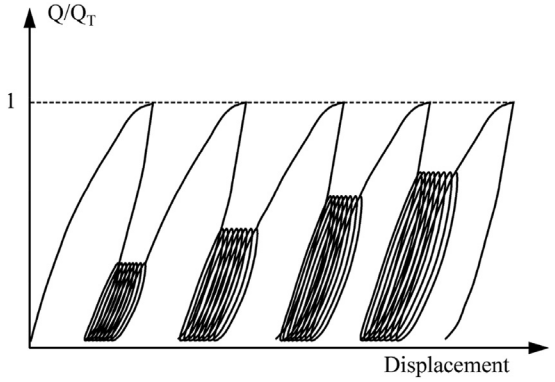

Fig. 1. Cyclic test programme for anchor 1CHA.

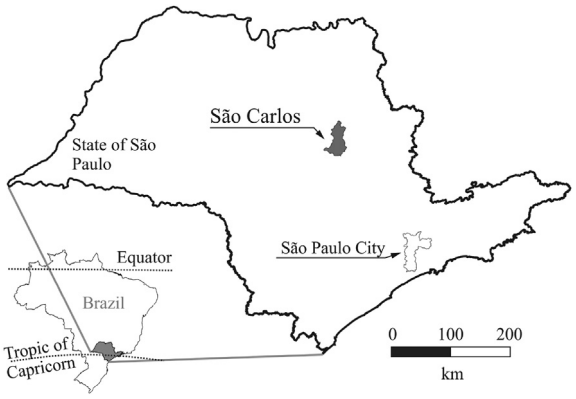

Fig. 2. São Carlos location.

The typical geotechnical-geologic profile of the experimental site includes a reddish clayey sand stratum originating from Mesozoic sandstones, overlaid by a 6 m thick brown clayey sand layer originating from Cenozoic sediments. Weathering in local conditions induced soil laterisation, which resulted in a very porous and collapsible material in superficial layer. A line of quartz pebbles and limonite is found separating the two soil layers. The groundwater table depth (GWT) varies seasonally between 9 m and 12 m.

Fig. 3 illustrates the soil horizontal variability at the experimental site, which was plotted from the results of standard penetration and cone penetration tests (SPT and CPT). At the helix depth (15 m), N_{SPT} (N_{60}) values are found to vary between 5 and 15 blows/(30 cm), while q_c values vary between 2 MPa and 3.3 MPa. This figure also illustrates the installation depth of the helical anchors tested in the current work.

2.2. Single-helix anchors

The lead section of the two identical single-helix anchors tested in this work was composed of a tubular steel shaft with external diameter of 101.6 mm and wall thickness of 7.1 mm, and a helical bearing plate with diameter of 305 mm, plate thickness of 12.5 mm and a pitch of 75 mm (Fig. 4). The helical anchors were instrumented with strain gauges oriented in Wheatstone full bridge to measure the axial force in a shaft section 250 mm above the helix. The strain gauges were unidirectional polyamide based model, the bondable type with a nominal resistance of 350 Ω, which are made out of designed steel.

The cables connecting the instrumented section to the data acquisition system were placed inside the anchor shaft. The hole to pass the cables as well as the circuit after adequate isolation was both sealed with adhesive joints. A split steel sleeve was used to cover the instrumentation to prevent damage using internal rubber rings and adhesive joints.

The instrumented sections of both anchors were calibrated using a load cell with the capacity of 500 kN and resolution of 0.02 kN, a hydraulic actuator attached to a manual hydraulic pump, and a steel reaction frame (Fig. 5). Data acquisition was performed using a portable data acquisition system, recording the electrical signals of both load cell and instrumentation.

2.3. Anchor installation

Each helical anchor was installed into the ground by applying mechanical torque at the anchor top with a hydraulic torque motor mounted on a backhoe loader. The installation torque was monitored with a digital torque indicator, as illustrated in Fig. 6. The

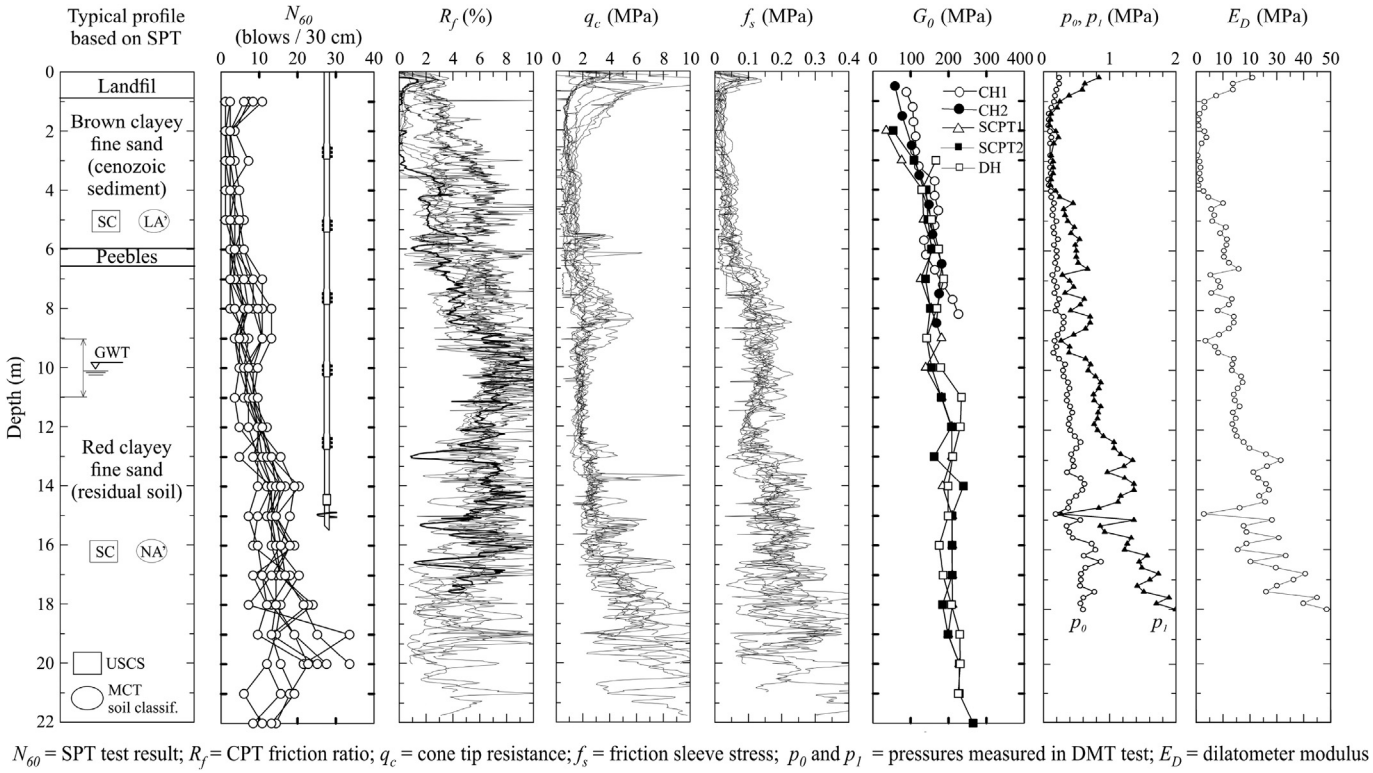

Fig. 3. Soil profile at the experimental site of the University of São Paulo at São Carlos, Brazil, after Giacheti et al. (2006a, b) (adapted).

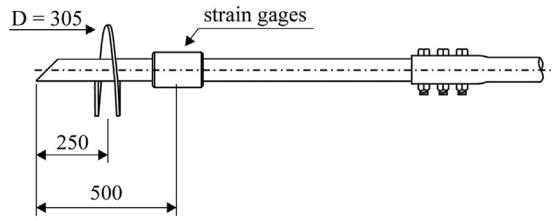

Fig. 4. Instrumented lead section of the helical anchors tested (dimensions in mm).

anchors were installed to a helix embedment depth of 15 m (as indicated in Fig. 3). Fig. 6 shows the equipment used for the helical anchor installation and the torque indicator in detail.

Results of torque readings are presented in Fig. 7 and are compared with the values reported by Tsuha (2007). Tsuha (2007) tested two double-helix anchors with smaller shaft diameter installed at the same site at an embedment depth of 14.4 m. Fig. 7 shows that the two identical helical anchors tested in the current investigation (1MHA and 1CHA) presented very similar results of installation torque along the depth, indicating that these anchors were installed in the same soil conditions and, for this reason, the results from tests on both anchors can be reliably compared.

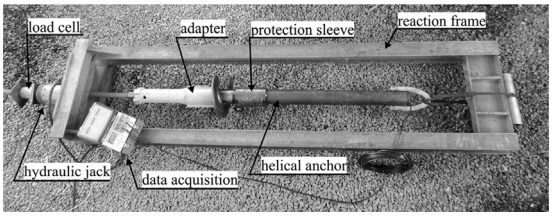

Fig. 5. Calibration of the instrumented lead section.

2.4. Load test setup

The monotonic and cyclic load tests in tension were performed using a hollow hydraulic jack with 450 kN capacity, and a reaction beam composed of two 2.7 m long steel I-beams W530 × 92 centred over the anchor and resting on wood cribbing. A threaded rod was used to connect the hydraulic jack to an adapter attached to the shaft top. The applied tensile load was measured with a 500 kN capacity load cell. The measurements of both load cell and instrumented section were registered every 15 s with the same portable data acquisition system used for calibration of the instrumented

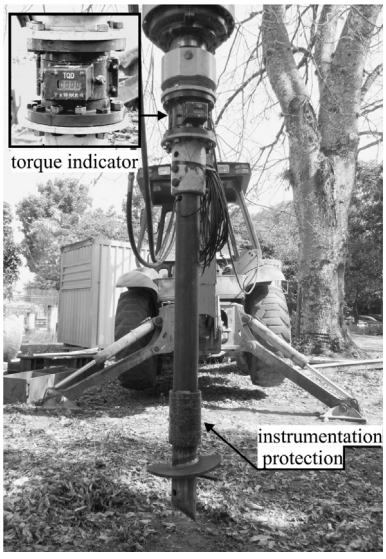

Fig. 6. Installation of an instrumented helical anchor at the test site.

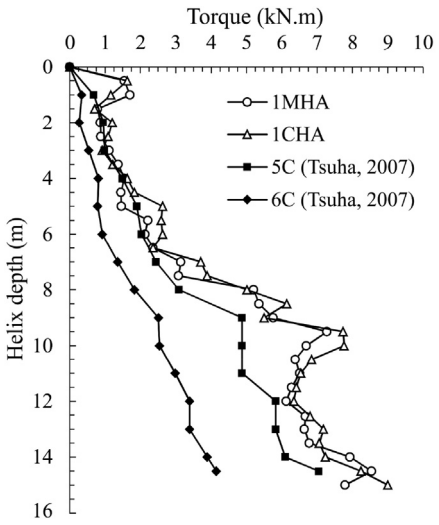

Anchor	Number of helices	$D_{lower\ helix}$ (mm)	$D_{upper\ helix}$ (mm)	d (mm)	H_{lower} (m)
1MHA	1	305	-	101.6	15.0
1CHA	1	305	-	101.6	15.0
5C	2	254	304.8	73.0	14.4
6C	2	127	152.4	73.0	14.4

Fig. 7. Results of installation torque obtained in the current investigation and those in Tsuha (2007).

sections. The anchor head displacements were monitored using four dial gauges with a resolution of 0.01 mm attached to two independent reference beams, and the readings were recorded every 30 s. Fig. 8 shows the load test setup.

Table 1
Programme of load tests performed on the anchors 1MHA and 1CHA.

Test No.	1CHA		1MHA	
	Test	Type of test	Test	Type of test
1	1M-test	Monotonic	1M-test	Monotonic
2	1C-test	Cyclic	2M-test	Monotonic
3	2M-test	Monotonic	3M-test	Monotonic
4	2C-test	Cyclic	4M-test	Monotonic
5	3M-test	Monotonic	5M-test	Monotonic
6	3C-test	Cyclic	–	–
7	4M-test	Monotonic	–	–
8	4C-test	Cyclic	–	–
9	5M-test	Monotonic	–	–

2.5. Load test procedure

The anchor designated as 1CHA was tested monotonically and cyclically. Firstly, the anchor 1CHA was subjected to a monotonic tensile load test, and then, 4 cyclic and 4 monotonic tests were performed in an alternate fashion. Such a test strategy was used to evaluate whether cycling affects the monotonic post-cyclic behaviour of the helical anchor installed in this particular site of residual soil. After the load tests on anchor 1CHA, 5 monotonic tensile load tests were performed on the reference anchor 1MHA for comparison purposes. These comparisons between the monotonic tests results of 1CHA and 1MHA show the effect of a previous cyclic loading on the anchor monotonic response related to the total capacity, in terms of helix bearing and shaft resistances. Table 1 summarises the loading tests carried out on both the instrumented helical anchors.

Prior to the monotonic tests, a seating load of 4 kN was applied to the anchors to eliminate slacks in the couplings of the shaft extension segments. The monotonic load tests were conducted

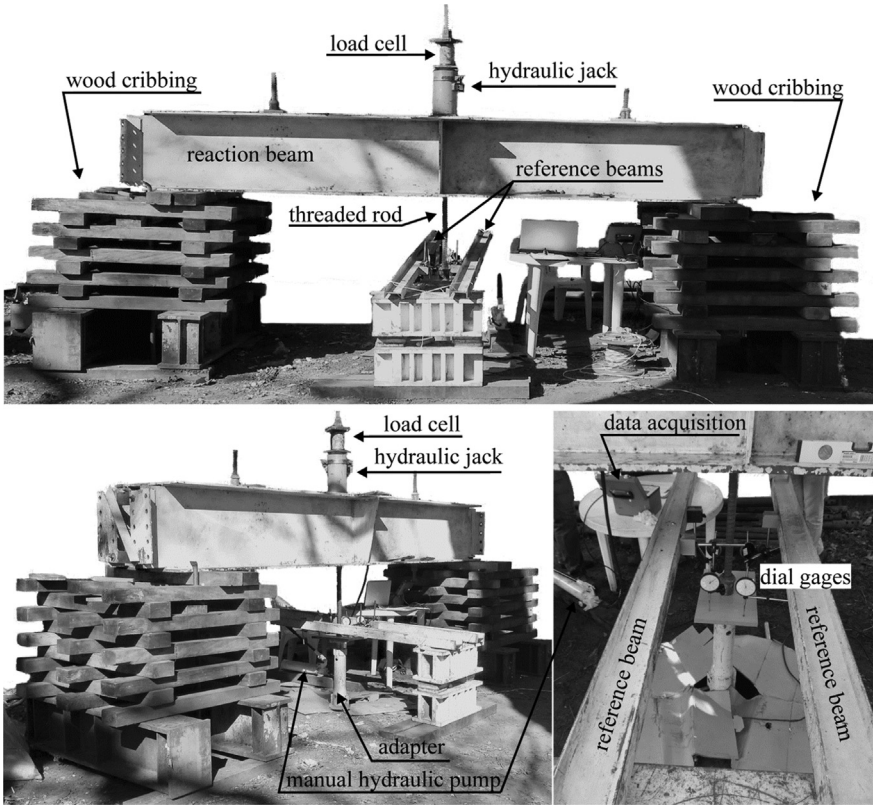

Fig. 8. Load test setup.

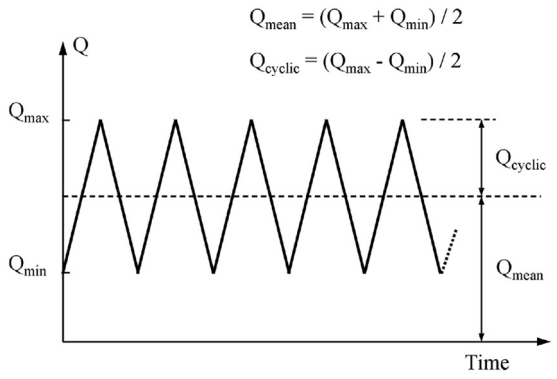

Fig. 9. Loading path and parameters of cyclic tests.

according to the Brazilian standard NBR-12131:2006 (2006). The load was applied in increments of 5% of the estimated ultimate uplift capacity by maintaining the loading for 5 min for each loading step (time interval accepted for special cases such as foundations of transmission towers). The loading stage continued up to an anchor head displacement equal to or greater than 0.1*D*.

An unloading stage was conducted following the loading stage for every monotonic load test. The unloading stage is a part of the load test procedure standardised by NBR-12131:2006 (2006). At the end of the unloading stage, permanent and recoverable displacements are possible to be separated, thereby providing more information on the anchor behaviour. In addition, for the anchor CHA1, the unloading stage is required to make the applied load reach the initial value (Q_{min}) for the cyclic test that follows.

The unloading stage was divided into 5 steps. The time step in the unloading stage was similar to that in the loading stage, except for the last unloading step, which was maintained for 60 min. In the last unloading step, the applied load is reduced up to 10% of the ultimate tensile load of the first monotonic test (Q_{T1}), which also corresponds to the minimum load for the cyclic tests (Q_{min}).

The loading path and parameters used to define the cyclic tests are illustrated in Fig. 9. The cyclic tests followed an approximately linear loading path, whose characteristics are listed in Table 2. In this table, Q_{T1} is the ultimate load in 1M-test, Q_{T2} is the ultimate load in 2M-test, Q_{T3} is the ultimate load in 3M-test, and Q_{T4} is the ultimate load in 4M-test. All the cyclic load tests were carried out with the same Q_{min}, which corresponded to $0.1Q_{T1}$ for the anchor 1CHA. The applied load was recorded every 25 s, and the anchor head displacement was measured twice per cycle (at Q_{max} and Q_{min}).

3. Results and discussion

3.1. Monotonic load-displacement response

Fig. 10 presents the load-displacement response of the first load test performed on both anchors 1MHA and 1CHA. Despite the seating load applied before the load test, the displacement was significantly larger in the first load increment for both anchors.

Table 2
Characteristics of the cyclic load tests on the anchor 1CHA.

Cyclic test	Q_{min} (kN)	Q_{max} (kN)	Number of cycles	Period (s)
1C-test	9.8 ($0.1Q_{T1}$)	19.5 ($0.2Q_{T1}$)	50	60
2C-test	9.8 ($0.06Q_{T2}$)	39 ($0.25Q_{T2}$)	50	60
3C-test	9.8 ($0.05Q_{T3}$)	58.6 ($0.32Q_{T3}$)	50	60
4C-test	9.8 ($0.05Q_{T4}$)	103.5 ($0.49Q_{T4}$)	50	60

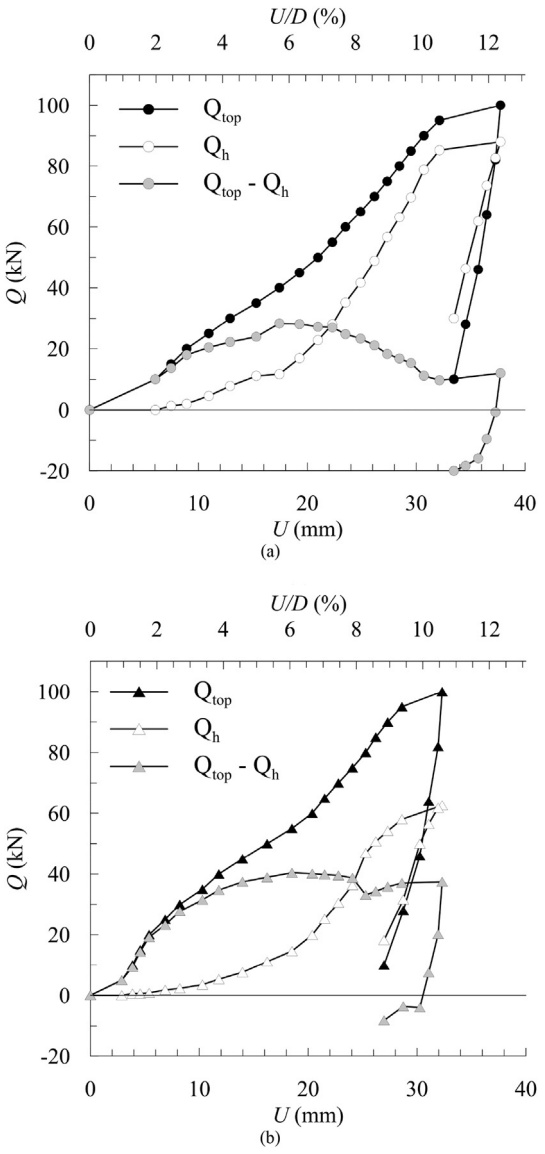

Fig. 10. Results of 1M-test performed on anchors (a) 1MHA and (b) 1CHA.

Similarly, Cerato and Victor (2009) reported the results of full-scale load tests with a significant anchor movement at the initial loading step that corresponded to $0.1Q_T$–$0.2Q_T$. According to Cerato and Victor (2009), this large anchor movement observed in the tests cannot be ascribed solely to the slack in the couplings, since each coupling had a tolerance of approximately 16 mm. This important initial displacement may have been the consequence of excessive disturbance on the soil mass above the helix during installation.

Fig. 10 shows that, in the following loading steps, the load-displacement response exhibited an approximately linear behaviour with an indicative of a plunging failure at a load corresponding to a displacement of 0.1*D* approximately. The last loading step (100 kN for both tests) induced an upward displacement of 37.74 mm (0.124*D*) and 32.31 mm (0.106*D*) for 1MHA and 1CHA, respectively.

In the present work, the ultimate uplift capacity is assumed as the applied load causing anchor head displacement to equal 0.1*D* (30 mm). According to Lutenegger (2008), this method eliminates subjectivity in any graphical interpretation of a load-displacement curve and takes a value of load at a reasonably large relative

displacement to ensure plastic failure in most soils. In Brazil, guyed cable anchors are usually assumed to fail for permanent displacements exceeding 0.1D. Moreover, the standard IEC 60826: 2017 (2017) suggests 50 mm as the failure limit for guyed anchors.

The values of ultimate uplift capacity in the 1M-test (Q_{T1}) were 89.1 kN and 97.6 kN for anchors 1MHA and 1CHA, respectively. The peak shaft resistance ($Q - Q_h$, where Q_h is the helix uplift bearing capacity, and Q is the applied load) occurred approximately at displacements of 0.11d and 0.18d (d is the shaft diameter) for 1MHA and 1CHA, respectively. Thereafter, a decrease was noticed for both anchors, but more evident for 1MHA. The helix bearing response in both tests was evaluated by analysing the instrumentation data of the shaft section above the helix, which was considered as the load resisted by the helix bearing. Fig. 11a shows the helix bearing resistance normalised by the applied load on the anchor head (Q_h/Q) at the loading stage. With increasing loading, both anchors exhibited similar mobilization trend, although the anchor 1MHA showed greater helix bearing capacity. At failure, the helix bearing capacity of anchor 1MHA was 77.2 kN (0.87Q_{T1}), while the anchor 1CHA showed 60.3 kN (0.62Q_{T1}). Low shaft resistance and, consequently, significant helix bearing resistance are attributed to the destruction of the soil structure around the shaft during anchor installation. In addition, the steel sleeve to protect the strain gauge instrumentation may have further disturbed the soil around the shaft, which may cause a decrease in the shaft-soil contact.

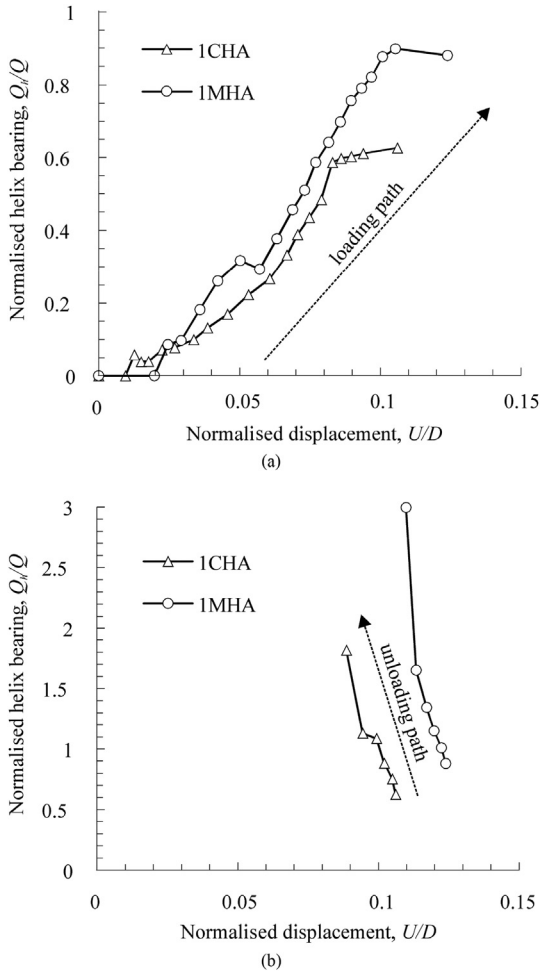

Fig. 11. Helix bearing resistance normalised by the applied load (Q_h/Q) at (a) loading and (b) unloading stages.

At the unloading stage, negative shaft friction and residual stresses at the helix were observed in both tests, with greater residual stresses for anchor 1MHA (Fig. 10). During the tensile loading stage, both skin friction and helix bearing resistances are acting downward to withstand the anchor uplift. But when the tensile load decreases at unloading stage, the bearing soil above the helix pulls the anchor back down, and at the same time, the anchor shaft recovers a portion of elastic elongation. These two components of rebound cause enough downward displacement to reverse the direction of skin friction in order to act upward, at least in the upper portion of the anchor shaft (Briaud and Tucker, 1984). Therefore, equilibrium is achieved when the skin friction shear stresses have reversed themselves in order to equilibrate the soil reaction forces acting on the helix.

Fig. 11b shows that the load in the instrumented section recognised as Q_h is greater than the applied load on the anchor head (Q) at the unloading stage. This means that a portion of the soil reaction force acting on the helix during the loading stage remains locked-in (residual stresses) at the unloading stage.

The pre-cyclic results were compared with the results of ultimate uplift capacity calculated by analytical and torque correlation methods. The analytical approaches chosen to predict the ultimate uplift capacity are the bearing plate model (Meyerhof and Adams, 1968), the approach proposed by Murray and Geddes (1987) and modified by Bagheri and El Naggar (2013), and the approach proposed by Pérez et al. (2018).

The bearing plate model assumes that soil failure occurs in a limited zone above the helix. The helix bearing capacity is calculated with the breakout factor F_q (Eq. (1)), which is expressed as a function of soil friction angle and helix embedment depth. Different proposals for F_q values can be found in the literature (e.g. Meyerhof and Adams, 1968; Mitsch and Clemence, 1985; Murray and Geddes, 1987; A.B. Chance Co., 2004). In the current study, F_q was determined based on the proposal of A.B. Chance Co. (2004) for helical anchors, which is an empirical modification of Meyerhof (1951)'s bearing capacity factors.

$$Q_T = Q_h = A_h \sigma' F_q \tag{1}$$

where A_h is the projected area of helix, and σ' is the effective vertical stress.

The approach proposed by Murray and Geddes (1987) and modified by Bagheri and El Naggar (2013) considered that failure develops along an inverted truncated cone-shaped surface above the helix. The anchor uplift capacity (Eq. (2)) is composed of a first component due to the shear resistance developed along the failure plane plus soil weight within the influence zone of failure (Eq. (3)), and a second component due to soil weight above the influence zone of failure (Eq. (4)).

$$Q_h = Q'_h + Q''_h \tag{2}$$

$$Q'_h = \gamma' A_h H' + \frac{2\gamma' A_h (H')^2}{D}\left\{1 + \frac{2H'}{3D}[\tan\theta + K\tan(\varphi' - \theta)]\right\} \tag{3}$$

$$Q'_h = \gamma'(H - H')\,\pi\,(0.5D + H'\tan\theta)^2 \tag{4}$$

where H is the helix embedment depth; H' is the height of influence zone in deep anchor behaviour, which is equal to 5D for bottom helix (or single-helix anchor); Q'_h is the helix uplift bearing component due to the shear resistance developed along the failure plane plus soil weight within the influence zone of failure; Q''_h is the helix uplift bearing component due to soil weight above the

influence zone of failure; K is the lateral earth pressure coefficient, which is assumed as passive lateral earth pressure coefficient (K_p) for anchors in dense sand (using residual friction angle), and as active lateral earth pressure coefficient (K_a) for anchors in loose sand; ϕ' is the internal friction angle of soil; γ' is the effective unit weight of soil; and θ is the angle between failure surface and the vertical, which is $22.5^\circ + \phi'/4$ for anchors in dense sand, and $22.5 - \phi'/4$ for anchors in loose sand.

Based on the observations of centrifuge tests and numerical modelling, the approach proposed by Pérez et al. (2018) assumed that the helix uplift bearing capacity (Q_h) corresponds to the mobilised shear resistance at the interface between the undisturbed soil and disturbed soil cylinder of 2.5D in length formed above the helix:

$$Q_h = \gamma' \left(H - \frac{h_0}{2} \right) K_u \tan\varphi'_{cv} \pi D h_0 \quad (5)$$

where h_0 is the length of the shear failure zone, which was assumed as 2.5D by Pérez et al. (2018); K_u is the lateral earth pressure coefficient in uplift proposed by Meyerhof and Adams (1968); and φ'_{cv} is the constant volume friction angle of soil.

In addition, the contribution of skin friction resistance to the anchor uplift capacity was estimated using Eq. (6) (Kulhawy, 1991). In the current study, the interface friction angle between the shaft and disturbed soil (δ) was considered equal to 10° (Tsuha et al., 2007).

$$Q_s = P_s \int_0^H K_u \sigma' \tan\delta \, dz \quad (6)$$

where P_s is the perimeter of shaft, Q_s is the skin friction capacity, and z is the depth.

The torque correlation method was presented in Hoyt and Clemence (1989). The uplift capacity of helical anchors can be estimated with the torque correlation factor K_T using the average installation torque (T_{avg}) measured at the final distance of penetration equal to 3D. For round shaft anchors in the diameter of 89 mm, Hoyt and Clemence (1989) proposed to use $K_T = 23\ m^{-1}$, and 9.8 m^{-1} for 219 mm diameter. Perko (2009) suggested using $K_T = 16\ m^{-1}$ for anchor shafts of 114 mm diameter. From a database of 30 load tests on multi-helix anchors with $d \approx 100$ mm installed in different sites in Brazil, Mosquera et al. (2016) found average K_T values of 12.8 m^{-1} and 20.1 m^{-1} for multi-helix anchors installed in clayey and sandy soils, respectively.

The soil properties used in estimation of anchor uplift capacity were obtained from previous research (Giacheti et al., 2006a). The internal friction angle of soil was determined with Mayne (2006)'s CPT correlation. Table 3 summarises the field results and predictions with the analytical methods. In general, the three methods overpredicted the helix bearing capacity. Better agreement was obtained with the method proposed by Pérez et al. (2018), which overpredicted the helix bearing capacity (48% and 13% for anchors 1CHA and 1MHA, respectively).

Table 3
Summary of field results and predictions of the analytical methods.

Anchor	T_{avg} (kN m)	K_T (m^{-1})	Q_h (kN)	Q_s (kN)
1CHA	8.16	12	60.3	–
1MHA	8.09	11	77.2	–
Bearing plate model	–	–	189.5	–
Bagheri and El Naggar (2013)	–	–	208.3	–
Pérez et al. (2018)	–	–	89.1	–
Kulhawy (1991)	–	–	–	65.2[a]/27.3[b]

[a] Skin friction capacity calculated separately from the bearing plate model using Eq. (6) and K_u values proposed by Mitsch and Clemence (1985).
[b] Skin friction capacity calculated using Eq. (6) and K_u equal to the Rankine's active lateral earth pressure coefficient (K_a).

Both the bearing plate model and Bagheri and El Naggar (2013)'s approach resulted in significantly large helix bearing capacity. The over-estimation induced by the two approaches may indicate that the ultimate uplift capacity given by the 0.1D failure criterion does not correspond to the ultimate limit state. That is, if an additional load increment was applied, the anchors could not exhibit an asymptotic trend of displacement increase and, therefore, this behaviour would not characterise the ultimate limit condition established in both the bearing plate model and Bagheri and El Naggar (2013)'s approach. In addition, the over-estimation induced by both methods may be indicative of severe soil disturbance around the anchor caused by the installation of anchor, which also explains the low values of shaft and helix bearing resistances.

Better prediction of the shaft resistance was obtained using K_u values equal to the Rankine's lateral active earth pressure coefficient (K_a) rather than using the K_u values calculated with Mitsch and Clemence (1985)'s recommendation.

The K_T values found for 1CHA (12 m^{-1}) and 1MHA (11 m^{-1}) are lower than the value proposed by Mosquera et al. (2016) for sandy soils (20.1 m^{-1}), but close to the value for clayey soils (12.8 m^{-1}). Perko (2009) suggested the K_T value of 16 m^{-1}, which is reasonably close to the values obtained in the current study. Although the average values of final torque lie within the range reported in the literature for single-helix anchors, the low K_T values are an indicator of the destruction of soil structure caused by the anchor installation. This means that a portion of soil strength due to the bonding structure is lost because of the helix penetration. Consequently, the helix bearing capacity in tension has only a portion of the installation torque, i.e. the amount of torque required to break the soil structure is not as low as the bearing capacity of the disturbed soil above the helix after installation.

3.2. Cyclic loading on anchor 1CHA

The results of both cyclic and subsequent monotonic load tests are presented in the same order in which the tests were conducted (chronological order). In addition, monotonic uplift tests were conducted on this anchor after each cyclic test. Fig. 12 presents the results of the four cyclic tests performed on the anchor 1CHA. The post-cyclic testing results will be discussed in Section 3.3.

Fig. 12a, b presents the results of the cyclic test carried out after the first monotonic uplift test on the anchor 1CHA (1C-test). The cyclic parameters of $Q_{min} = 0.1Q_{T1}$ and $Q_{max} = 0.2Q_{T1}$ were designated for the 1C-test to verify the potential for anchor capacity increase due to low-intensity cyclic loading, which corresponds to a typical service condition of load intensity in guyed tower anchors. Due to the monotonic load test conducted previously (1M-test), the cyclic loading caused only very small displacements (around 0.1D) at each cycle along with negative (downward) displacement accumulation (Fig. 12a).

Fig. 12b shows a decrease in Q_h during cycling (around 17% at the end of cycles), indicating that the direction of shear forces at the shaft-soil interface fluctuates between upward and downward depending on the magnitude of the force applied to the anchor. No degradation of helix bearing resistance was observed for numbers of cycles carried out due to improvement of the soil above the helix caused by the loading applied during the 1M-test. Thus, the decrease in Q_h is probably due to the reversal of skin friction, which leads to positive friction. As the reversal of skin friction occurs, the anchor rebound is no longer prevented, which makes the anchor accumulate negative displacement (downward).

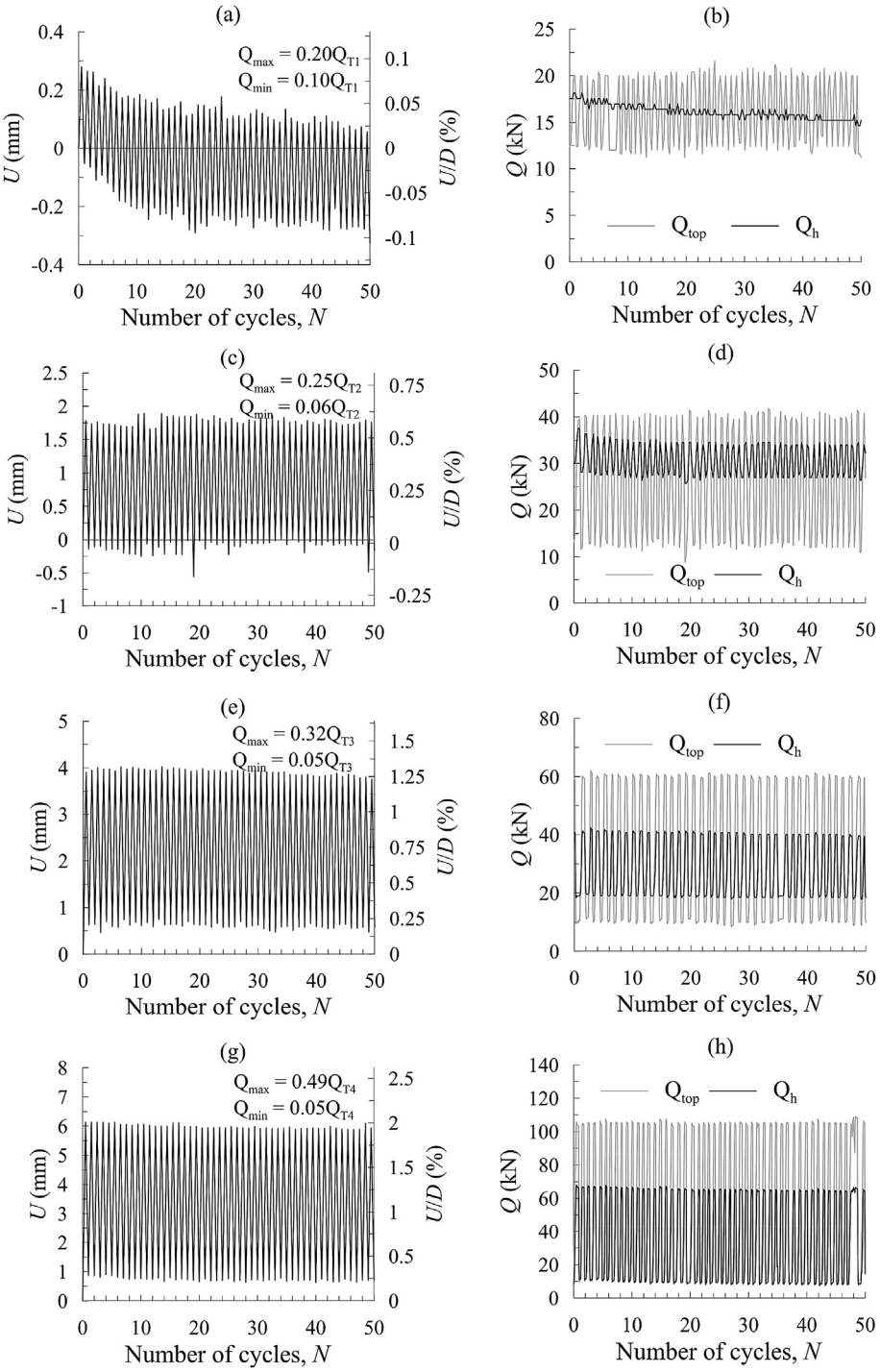

Fig. 12. 1CHA cyclic test results: (a, b) 1C-test; (c, d) 2C-test; (e, f) 3C-test; and (g, h) 4C-test.

After 2M-test, a second cyclic test (2C-test) was carried out with load amplitude of $0.19Q_{T2}$ (29 kN), and Q_{max} corresponding to $0.25Q_{T2}$ (Q_{T2} is the ultimate load in 2M-test). Fig. 12c shows that negligible displacement is accumulated with cycles, and Fig. 12d indicates a slight decrease in the maximum value of Q_h (approximately 12% decrease). Also in Fig. 12d, the minimum value of Q_h is observed to be greater than the minimum value of the applied load (Q_{min}), indicating that both negative skin friction and residual stresses at the helix still occur.

Fig. 12e, f shows that the 3C-test ($Q_{min} = 0.05Q_{T3}$ and $Q_{max} = 0.32Q_{T3}$, where Q_{T3} is the ultimate load in 3M-test) had negligible influence on the anchor performance. After an accumulated upward displacement of 0.62 mm at the first cycle, the anchor remained stable without displacement accumulation. In addition, no evident degradation of helix bearing resistance was noticed. The reason for the absence of displacement accumulation with cycles is likely the soil improvement above the helix caused by previous monotonic loading, which tends to stiffen the anchor response increasingly.

The percentage of load carried by helix bearing was less in the 3C-test than that in the 2C-test. While the 2C-test measured a maximum Q_h/Q of 94%, the 3C-test showed a maximum Q_h/Q of

71%, which indicates that: (i) the helix bearing reached its ultimate capacity, and (ii) the positive shaft friction resistance showed potential to further mobilisation. Moreover, Fig. 12f shows that Q_h values were less than Q throughout the 3C-test, which suggests that the direction of shear forces at the shaft-soil interface no longer changes with cycles.

Fig. 12g, h presents the results of the 4C-test, which was conducted with cyclic loading parameters of $Q_{min} = 0.05Q_{T4}$ and $Q_{max} = 0.49Q_{T4}$ (Q_{T4} is the ultimate load in 4M-test). Although the cyclic test was conducted with load amplitude 92% greater than that in the previous cyclic test, the anchor performance was similar. The first load cycle caused 1.5 mm of accumulated displacement in 4C-test, but no increase in accumulated displacement was observed in the subsequent cycles. In addition, negligible degradation of helix bearing resistance was noted.

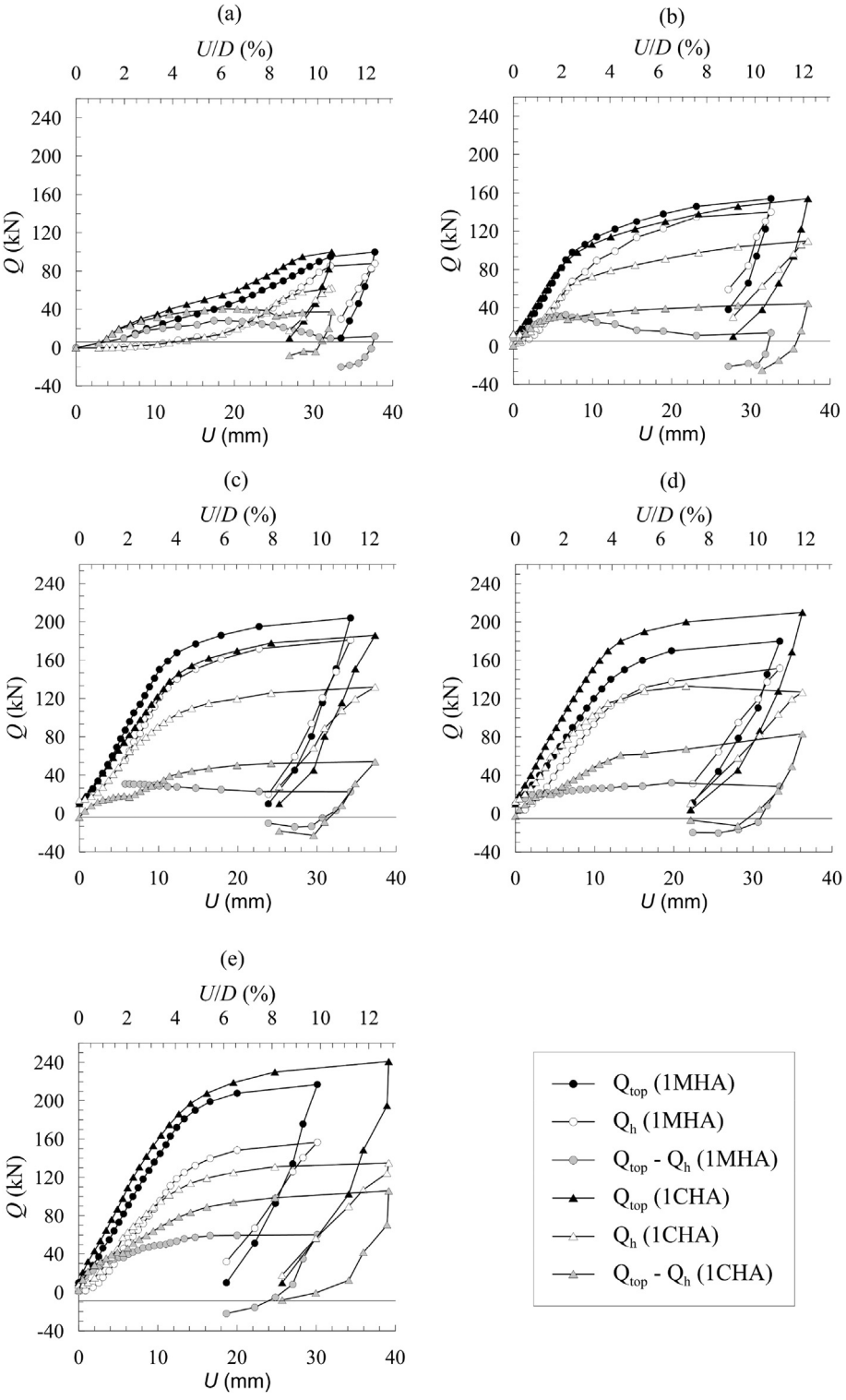

Fig. 13. Results of the monotonic tensile load tests: (a) 1M-test, (b) 2M-test, (c) 3M-test, (d) 4M-test, and (e) 5M-test.

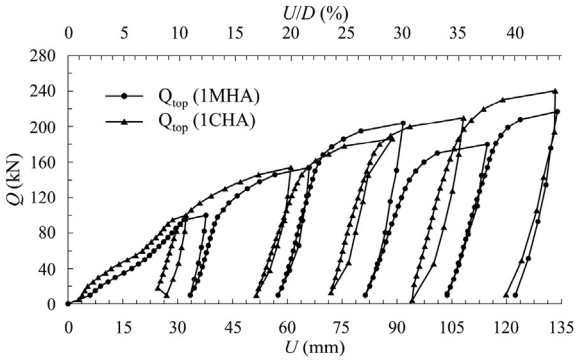

Fig. 14. Monotonic load-displacement responses plotted according to the movement history of each anchor.

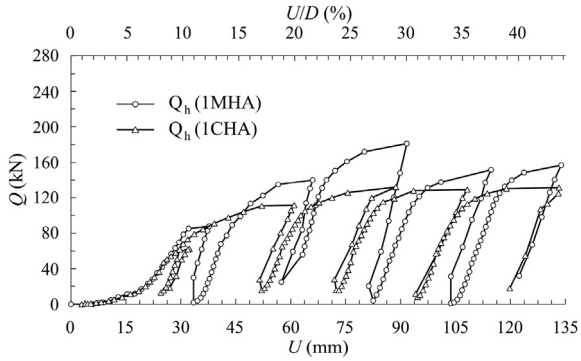

Fig. 15. Measured load in the instrumented section above the helix plotted according to the movement history of each anchor.

3.3. Post-cyclic monotonic response

The results of anchor 1MHA were taken as a benchmark since no cyclic load tests were performed on this anchor. The cyclic performance of anchor 1CHA was influenced by the preceding ultimate monotonic load, as shown in the previous section. In contrast, the cyclic loading was shown to have little or negligible influence on the monotonic response of anchor 1CHA.

The load-displacement response of the 1M-test differed significantly from that of the following monotonic tests for both anchors 1MHA and 1CHA (Fig. 13). However, this difference cannot be attributed to the influence of cycling because both anchors 1MHA and 1CHA showed similar shape of the load-displacement response in the subsequent monotonic test (2M-test). The approximately linear shape of the load-displacement response of the first monotonic test (1M-test) is the result of the volumetric strain of the soil in the zone above the helix, which is accompanied by large anchor displacement and increases in strength and stiffness. On the other hand, the load-displacement response of the subsequent monotonic test (2M-test) exhibits a stiffer linear portion with little displacement up to the load value applied in the previous load test approximately, which represents recompression behaviour (Fig. 13b).

The 2M-test showed differences in the behaviour of Q_s and Q_h for both anchors (Fig. 13b). While anchor 1MHA exhibited a peak and then decreased for Q_s, no post-peak decrease was noticed for anchor 1CHA in 2M-test. At failure, greater Q_h for anchor 1MHA ($0.91Q_T$) than that for anchor 1CHA ($0.72Q_T$) was observed.

For the following monotonic load tests (3M-test, 4M-test and 5M-test), three different trends were noticed in the load-displacement response: a first linear portion starting from zero up to an upward displacement between $0.03D$ and $0.04D$, followed by a nonlinear portion up to around $0.07D$ upward displacement, and then an indicative of plastic failure with asymptotic trend (Fig. 13c–e). As in 2M-test, no clear influence on the post-cyclic ultimate capacity caused by the cyclic loading could be inferred, although the greater ultimate uplift capacity observed for 1CHA than that for 1MHA in both 3M-test and 4M-test may suggest that some capacity increase was caused by the load cycles.

Table 4
Summary of the results of the monotonic uplift load tests.

Test	1MHA			1CHA		
	Q_T (kN)	Q_h (kN)	Q_s (kN)	Q_T (kN)	Q_h (kN)	Q_s (kN)
1M-test	89.1	77.2	11.9	97.6	60.3	37.3
2M-test	154	140	14	154	111.3	42.7
3M-test	204	181	23	186	131.9	54.1
4M-test	180	151.5	28.5	210	129	81
5M-test	217	156.7	60.3	241	131.1	109.9

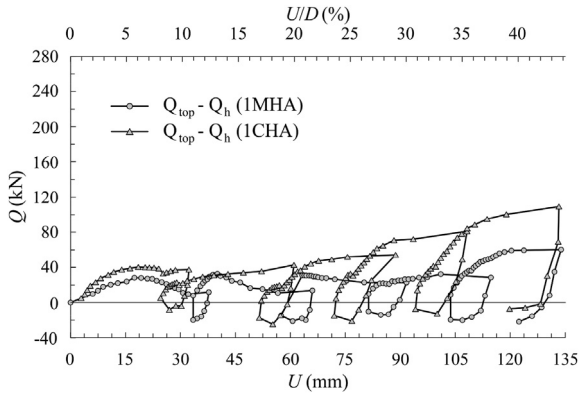

Fig. 16. Skin friction plotted according to the movement history of each anchor.

Concerning the effects of applying a single ultimate load cycle on the anchor ultimate capacity, i.e. a monotonic load test, no ultimate capacity degradation was noticed for both anchors 1MHA and 1CHA at a subsequent monotonic test. Each time when the anchors were re-tested monotonically, the ultimate load capacity was greater. When the load-displacement responses were plotted according to the movement history, each monotonic test appeared to continue once the preceding test was completed, sometimes with some capacity increase for anchor 1CHA (Fig. 14). Table 4 summarises the results of the monotonic load tests on both anchors 1MHA and 1CHA.

Figs. 15 and 16 show Q_h and Q_s in all monotonic tests according to the movement history, respectively. At failure, both Q_h and Q_s increased with each monotonic test (Table 4), although a slightly greater increase in Q_h was observed for the anchor subjected only to monotonic loading (1MHA). In contrast, greater increase in Q_s was noticed for the anchor that experienced cyclic loading (1CHA). Moreover, Figs. 12b, d, f, h and 16 suggest that both negative skin friction and residual stresses at the helix are reduced after a series of cyclic loading.

4. Conclusions

Monotonic, cyclic and post-cyclic tensile load tests were performed on two instrumented single-helix anchors installed in residual tropical soil. The post-cyclic test results were compared with those of a benchmark anchor subjected only to monotonic load tests. The main findings of the current study are listed as follows:

(1) Values of torque correlation factor K_T in the current study are significantly lower in comparison with values obtained with single-helix anchors of similar dimensions. This is because the installation torque is a function of undisturbed soil (shear strength associated with the undisturbed bonded structure), and the uplift capacity depends on the disturbed soil.
(2) The soil improvement above the helix caused by previous monotonic loading increased the anchor axial stiffness. Consequently, plastic deformations in the zone above the helix were minimised, no displacement accumulation occurred at any cyclic test, and only elastic displacements were observed.
(3) The influence of cyclic loading on the post-cyclic capacity could not be clearly observed in all post-cyclic tests. In comparison with the benchmark anchor, only after cyclic tests with larger amplitude (3C-test and 4C-test), some increase in the post-cyclic capacity was observed. This increase in capacity is mainly attributed to the increase in the shaft resistance since similar helix bearing capacity was observed for the three last monotonic tests on anchor 1CHA.
(4) Although both helix bearing and shaft resistances increased due to previous monotonic tests, the cyclically tested anchor exhibited greater increase in shaft resistance. On the other hand, a slightly greater increase in helix bearing resistance was noticed for the anchor subjected only to monotonic loading.
(5) From a design point of view, the current study indicates that the soil disturbance by the anchor installation has a major influence on the initial stiffness of the tested anchors in residual soil. Therefore, results from theoretical prediction methods should be used with caution since displacements larger than 0.1D were experienced by the anchors without characterising the ultimate limit state. In addition, a rapid monotonic loading procedure up to the predicted uplift capacity can reduce the cyclic displacement accumulation of helical anchors in residual soils. However, a site-specific field validation campaign should be conducted.

Conflicts of interest

The authors wish to confirm that there are no known conflicts of interest associated with this publication and there has been no significant financial support for this work that could have influenced its outcome.

Acknowledgements

This study was financed in part by the Coordenação de Aperfeiçoamento de Pessoal de Nível Superior, Brazil (Finance Code 001) and the USP-COFECUB Project (Grant No. UcMa 132/12). The authors appreciate the valuable assistance provided by the colleagues at the Department of Geotechnical Engineering, University of São Paulo (USP), mainly by the PhD candidate J. Santos Filho.

References

Bagheri F, El Naggar MH. Effects of installation disturbance on behavior of multi-helix anchors in sands. In: Proceedings of the 66th Canadian geotechnical conference (GeoMontreal 2013). Montréal, Canada. Canadian Geotechnical Society (CGS); 2013. Paper No. 242.
Bagheri F, El Naggar MH. Effects of installation disturbance on behavior of multi-helix piles in structured clays. DFI Journal – The Journal of the Deep Foundations Institute 2015;9(2):80–91.
Briaud JL, Tucker L. Piles in sand: a method including residual stresses. Journal of Geotechnical Engineering 1984;110(11):1666–80.
Buhler R, Cerato AB. Design of dynamically wind-loaded helical piers for small wind turbines. Journal of Performance of Constructed Facilities 2010;24(4):417–26.
Cerato AB, Victor R. Effects of long-term dynamic loading and fluctuating water table on helical anchor performance for small wind tower foundations. Journal of Performance of Constructed Facilities 2009;23(4):251–61.
A.B. Chance Co.. Helical pier foundation systems. Technical Manual Bulletin 01-9601 2004.
Clemence SP, Smithling AP. Dynamic uplift capacity of helical anchors in sand. In: Geomechanics-interaction, Proceedings of the 4th Australia-New Zealand Conference on Geomechanics. Australian Geomechanics Society and New Zealand Geomechanics Society; 1984. p. 88–93.
Costa JPS. Uplift behaviour of helical piles in sand subjected to cyclic loading. MSc Thesis. Natal, Brazil: Federal University of Rio Grande do Norte; 2017.
Fahmy A, El Naggar MH. Cyclic axial performance of helical-tapered piles in sand. DFI Journal - The Journal of the Deep Foundations Institute 2016;10(3):98–110.
George D, Clemence SP. Effects of installation disturbance on elastic modulus for helical anchor short-term uplift loading in clay. In: Proceedings of the 1st international geotechnical symposium on helical foundations. Amherst, USA: International Society for Helical Foundations; 2013. p. 8–10.
Giacheti HL, De Mio G, Peixoto ASP. Cross-hole and seismic CPT tests in a tropical soil site. In: DeGroot DJ, DeJong JT, Frost D, Baise LG, editors. Proceedings of GeoCongress 2006: geotechnical engineering in the information age. American Society of Civil Engineers (ASCE); 2006a. https://doi.org/10.1061/40803(187)92.
Giacheti HL, Peixoto ASP, De Mio G, Carvalho D. Flat dilatometer testing in Brazilian tropical soils. In: Proceedings of the 2nd international flat dilatometer conference. Washington D.C., USA: International Society for Soil Mechanics and Geotechnical Engineering (ISSMGE); 2006b. p. 103–10.
Hoyt RM, Clemence SP. Uplift capacity of helical anchors in soil. In: Proceedings of the 12th international conference on soil mechanics and foundation engineering. Rotterdam: A.A. Balkema; 1989. p. 1019–22.
IEC 60826:2017. Design criteria of overhead transmission lines. Geneva, Switzerland: International Eletrotechnical Commission (IEC); 2017.
Kulhawy FH. Uplift behaviour of shallow soil anchors - an overview. In: Clemence SP, editor. Uplift behavior of anchor foundations in soil. ASCE; 1985. p. 1–25.
Kulhawy FH. Drilled shaft foundations. In: Fang HY, editor. Foundation engineering handbook. Boston, USA: Springer; 1991. p. 537–52.
Lutenegger AJ. Tension tests on single-helix screw piles in clay. In: Proceedings of the 2nd British geotechnical association international conference on foundations. Scotland, UK: IHS BRE Press; 2008. p. 201–12.
Lutenegger AJ, Tsuha CHC. Evaluating installation disturbance from helical piles and anchors using compression and tension tests. In: Proceedings of the 15th pan-American conference on soil mechanics and geotechnical engineering. Amsterdam, the Netherlands: IOS Press; 2015. p. 373–81.
Mayne PW. The Second James K. Mitchell Lecture: undisturbed sand strength from seismic cone tests. Geomechanics and Geoengineering 2006;1(4):239–57.
Meyerhof GG. The ultimate bearing capacity of foundations. Geotechnique 1951;2(4):301–32.
Meyerhof GG, Adams JI. The ultimate uplift capacity of foundations. Canadian Geotechnical Journal 1968;5(4):225–44.
Mitchell JK, Sitar N. Engineering properties of tropical residual soils. In: Engineering and construction in tropical and residual soils, proceedings of the ASCE geotechnical engineering division specialty conference. Honolulu, USA: ASCE; 1982. p. 30–57.
Mitsch MP, Clemence SP. The uplift capacity of helix anchors in sand. In: Clemence SP, editor. Uplift behavior of anchor foundations in soil. ASCE; 1985. p. 26–47.
Mosquera ZZ, Tsuha CHC, Beck AT. Serviceability performance evaluation of helical piles under uplift loading. Journal of Performance of Constructed Facilities 2016;30(4). https://doi.org/10.1061/(ASCE)CF.1943-5509.0000805.
Murray E, Geddes J. Uplift of anchor plates in sand. Journal of Geotechnical Engineering 1987;113(3):202–15.
Nagata M, Hirata H. Study on uplift resistance of screwed steel pile. Nippon Steel Technical Report No. 92. Tokyo, Japan: Nippon Steel & Sumitomo Metal Corporation; 2005. p. 73–8.
Narasimha Rao S, Prasad Y. Behavior of a helical anchor under vertical repetitive loading. Marine Geotechnology 1991;10(3–4):203–28.
NBR 12131:2006. Piles – static load test – test method. Rio de Janeiro, Brazil: Brazilian Technical Standards Association (ABNT); 2006 (in Portuguese).
Newgard JT, Schneider JA, Thompson D. Cyclic response of shallow helical anchors in a medium dense sand. In: Proceedings of the 3rd conference on frontiers in offshore geotechnics. London, UK: A.A. Balkema; 2015. p. 913–8. https://doi.org/10.1201/b18442-131.
Pérez ZA, Schiavon JA, Tsuha CHC, Dias D, Thorel L. Numerical and experimental study on the influence of installation effects on the behaviour of helical anchors in very dense sand. Canadian Geotechnical Journal 2018;55(8):1067–80.
Perko HA. Helical piles: a practical guide to design and installation. Hoboken, USA: John Wiley & Sons; 2009.
Schiavon JA, Tsuha CHC, Thorel L. Cyclic and post-cyclic monotonic response of a single-helix anchor in sand. Géotechnique Letters 2017;7(1):11–7.
Schiavon JA, Tsuha CHC, Neel A, Thorel L. Centrifuge modelling of a helical anchor under different cyclic loading conditions in sand. International Journal of Physical Modelling in Geotechnics 2018. https://doi.org/10.1680/jphmg.17.00054.
Townsend FC. Geotechnical characteristics of residual soils. Journal of Geotechnical Engineering 1985;111(1):77–94.

Trofimenkov JG, Mariupolskii LG. Screw piles used for mast and tower foundations. In: Proceedings of the 6th international conference on soil mechanics and foundation engineering. Toronto, Canada: University of Toronto Press; 1965. p. 328–32.
Tsuha CHC. Theoretical model to control on site the uplift capacity of helical screw piles embedded in sandy soil. PhD Thesis. São Carlos, Brazil: University of São Paulo; 2007. p. 267 (in Portuguese).
Tsuha CHC, Aoki N, Rault G, Thorel L, Garnier J. Physical modelling of helical pile anchors. International Journal of Physical Modelling in Geotechnics 2007;7(4):1–12.
Tsuha CHC, Aoki N, Rault G, Thorel L, Garnier J. Evaluation of the efficiencies of helical anchor plates in sand by centrifuge model tests. Canadian Geotechnical Journal 2012;49(9):1102–14.
Tsuha CHC, Santos Filho JMSM, Costa Santos T. Helical piles in unsaturated structured soil: a case study. Canadian Geotechnical Journal 2016;53(1):103–17.
Wang D, Gaudin C, Merifield RS, Hu Y. Centrifuge model tests of helical anchors in clay. In: Proceedings of the 7th international conference on physical modelling in geotechnics. Zurich, Switzerland: CRC Press; 2010. p. 1069–74.
Weech C, Howie JA. Helical piles in soft sensitive soils – a field study of disturbance effects on pile capacity. In: VGS symposium on soft ground engineering. Vancouver, Canada: Vancouver Geotechnical Society (VGS); 2012. p. 1–11.
Wesley LD. Fundamentals of soil mechanics for sedimentary and residual soils. John Wiley & Sons; 2009.

José Antonio Schiavon is Adjunct Professor of Geotechnical Engineering at the Aeronautics Institute of Technology, São José dos Campos, Brazil. He obtained his PhD degrees from the University of São Paulo at São Carlos, Brazil, and from the École Centrale de Nantes, France. He was postdoctoral fellow at the University of São Paulo at São Carlos for two years (2016–2017). He has practical experience in numerical modelling, and laboratory centrifuge and field testing. His research interests are geosynthetics and foundations, with emphasis on mechanical behaviour, soil-structure interaction, cyclic loading, physical modelling, and laboratory and field tests.

Cristina de Hollanda Cavalcanti Tsuha is Associate Professor at the Department of Geotechnical Engineering at the University of São Paulo in Brazil. She graduated from the Mauá Institute of Technology (São Paulo, Brazil) in 1994. She worked as civil engineer in engineering companies during several years (1995–2001). She has been involved in different projects related to geotechnical site investigations, foundations, and earth structures. She has obtained her MSc and PhD degrees in Geotechnical Engineering from the University of São Paulo (2003 and 2007). Her main research interests cover foundations engineering, with emphasis on the following topics: (i) behaviour of pile and shallow foundations, (ii) pile foundations in unsaturated soils, (iii) physical modelling of pile behaviour in centrifuge and calibration chamber, (iv) geothermal energy piles, and (v) foundations under cyclic loading.

Luc Thorel is researcher of the Nantes Centre of the French Institute of Science and Technology for Transport, Development and Networks (IFSTTAR) to work on physical modelling in the Geotechnical Centrifuge team since 1996. In 2010, he became Director of Research in IFSTTAR. Luc Thorel's current research explores themes concerned with physical modelling in geotechnics, particularly with the geotechnical centrifuge. He is working mainly on soil-structure interactions under complex loading, such as soil reinforcement, deep and shallow foundations but also on water migration in soil (including soil-atmosphere interactions or erosion) or vibration mitigation. The ongoing challenge for each of these topics is to observe and understand the phenomena, and also to obtain appropriate experimental data to be compared to numerical or theoretical models.